HTD-Vol. 305

Proceedings of the 30th

1995 NATIONAL HEAT TRANSFER CONFERENCE

VOLUME 3

- HEAT TRANSFER IN MICROGRAVITY SYSTEMS
- FUNDAMENTALS OF THREE-DIMENSIONAL NATURAL CONVECTION
- MICROCHANNEL HEAT TRANSFER

presented at

THE 1995 NATIONAL HEAT TRANSFER CONFERENCE
PORTLAND, OREGON
AUGUST 6–8, 1995

sponsored by

THE HEAT TRANSFER DIVISION, ASME

edited by

S. S. SADHAL
UNIVERSITY OF SOUTHERN CALIFORNIA

A. GOPINATH
NAVAL POSTGRADUATE SCHOOL

PATRICK H. OOSTHUIZEN
QUEENS UNIVERSITY

AB HASHEMI
LOCKHEED MARTIN

THE AMERICAN SOCIETY OF MECHANICAL ENGINEERS
United Engineering Center • 345 East 47th Street • New York N.Y. 10017

CONTENTS

STUDY OF VAPOR BUBBLE GROWTH IN SUPERSATURATED LIQUID

J. Straub, J. Winter, G. Picker
Lehrstuhl A für Thermodynamik, TU München
Arcisstr. 21, 80290 München, Germany

M. Zell
DASA GmbH, Dornier
88039 Friedrichshafen

ABSTRACT

Experiments for the investigation of the evaporation and condensation kinetics at the phase interface of single vapor bubbles have been performed under microgravity conditions. The bubble growth rates for bubbles growing in a homogeneous supersaturated liquid could be determined from films obtained during the experiments. A numerical model for the calculation of the bubble growth controlled by heat conduction has been developed. The calculated growth rates are in good agreement with the measured one. Finally the evaporation and condensation coefficients for the refrigerant R11 are determined.

INTRODUCTION

The evaporation and condensation process is very important for many technical applications in chemical engineering and power conversion. For example the boiling mechanism, which is governed by the evaporation and condensation process, is a very efficient method for heat transfer with a high heat flux density. The boiling heat transfer under microgravity as well as under normal gravity is strongly influenced by the evaporation and condensation process. The boiling heat transfer coefficients are usually described by empirical equations with a very limited range of validity. For a more general description of the boiling heat transfer a better understanding of the evaporation and condensation process is necessary. Therefore this experimental work focuses on vapor bubble growth and vapor bubble collapse in a supersaturated liquid with an initial uniform temperature field. The bubble growth and collapse is referred to in general as bubble dynamics. To overcome the problems of former experimental works (/1/ and /2/) like short times of observation and non-uniform temperature fields around the bubbles, we decided to perform experiments under microgravity conditions.

In July 1994 we flew an experiment on the IML 2 mission of NASA. The experiment was conducted in the BDPU (**B**ubble **D**rop and **P**article **U**nit), which is a multiuser facility for fluid physics experiments in space, built and operated under the responsibility of ESA (**E**uropean **S**pace **A**gency). During the research project we could perform further experiments in the Japanese drop shaft (JAMIC), in the German drop tower and during a sounding rocket flight. At the time when this paper was written, the data base of the Spacelab experiment was not yet completed and evaluated. Therefore only the results of the pre experiments, carried out at low Jakob Numbers, are summarized in this paper.

To conduct these experiments the pressure of an isothermal liquid was reduced below the saturation pressure of the liquid, in order to achieve an isothermal supersaturated liquid. The bubbles were generated by a short heating pulse of a spot heater. In the absence of earth gravity the bubbles remain at the place of nucleation and grow in an undisturbed temperature field. The driving force for bubble growth (evaporation) and for bubble shrinkage (condensation) in the isothermal supersaturated or subcooled liquid with uniform liquid temperature is the temperature difference between the liquid vapor interface and the surrounding liquid. Heat conduction is responsible for the transport of the latent heat needed for evaporation and condensation. The bubble growth rates are calculated with a numerical model based on the conservation equations for the liquid around growing vapor bubbles

The evaporating and condensing mass flow over the liquid vapor interface can also be described by using the equations of the kinetic theory, taking into account the small temperature jump at the liquid vapor interface. Usually the experimental mass flow rate is lower than the one predicted by the kinetic theory.

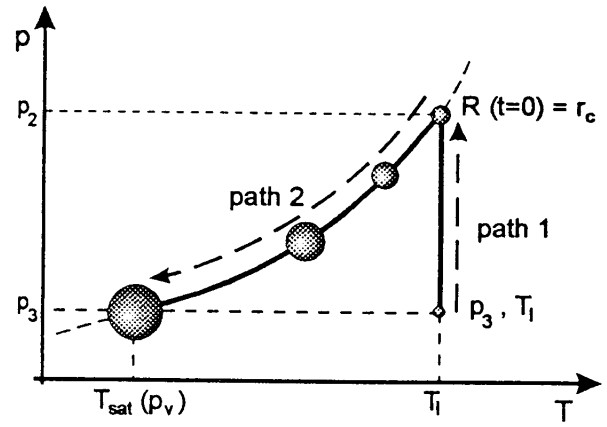

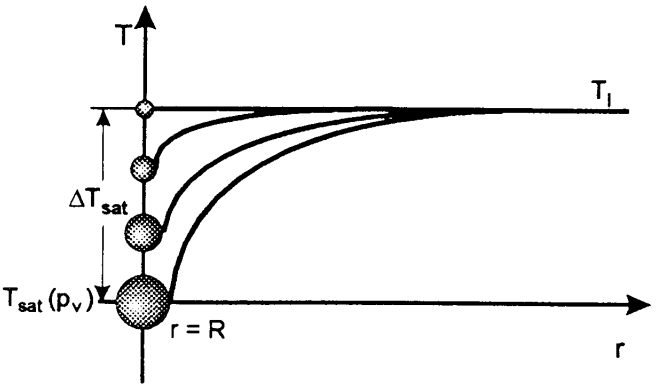

Fig. 2: a) Bubble Growth on the p,T phase diagram b)Temperature field around the bubble

Therefore the evaporation and the condensation coefficients were introduced, representing the ratio of the measured mass flow rate to the theoretical one. Beside the comparison of the experimental results with the above mentioned model we were also able to calculate the accommodation coefficients from the results obtained with the experiments.

BUBBLE GROWTH IN SUPERSATURATED LIQUID

The Thermodynamic Process

In the boiling process usually the bulk liquid near a heater is superheated at a constant liquid pressure. The result is a growing vapor bubble in a non-uniform temperature field. In our experiments a liquid with uniform temperature was supersaturated by reducing the pressure nearly isothermal below the saturation pressure of the liquid.

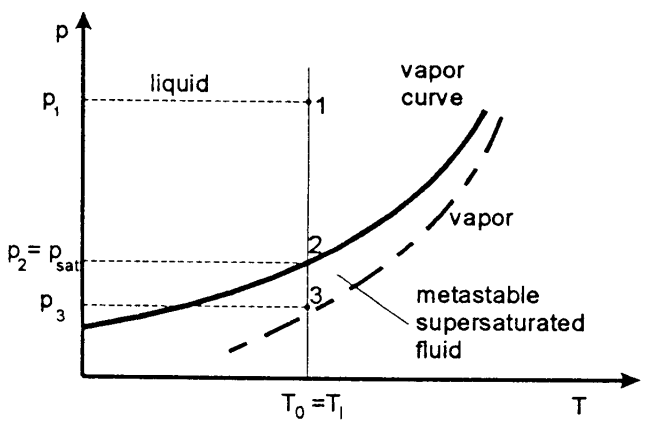

Fig. 1: Thermodynamic process shown on a p,T phase diagram

The principle thermodynamic process is shown in fig. 1, a p,T - phase diagram of FREON R11, which was used as a model fluid. The pure and degassed R11 is heated to and maintained at a constant temperature T_0. By increasing the pressure above saturation to p_1 (fig. 1, state 1), vapor nuclei on the surface of the cell walls are inactivated down to a distinct size given by the following equation. In this equation r is the smallest nucleus to be deactivated.

$$r = \frac{2\sigma}{\Delta p} = \frac{2\sigma}{p_1 - p_2} \qquad (1)$$

The isothermal supersaturated liquid is achieved by reducing the pressure of the liquid to a pressure p_3 below the saturation pressure $p_2 = p_{sat}$, corresponding to the liquid temperature. In this metastable state, vapor bubbles are generated by a short heating pulse of a thermistor used as miniaturized heater. The nucleation of the bubbles is shown as **path 1** in fig. 2a. The radius of the activated bubbles is equal to a critical radius, which can be calculated with the pressure difference p_2 - p_3 by using eq. (1). In the following period (**path 2**, fig. 2a) the bubble growth is controlled by the pressure difference between the bubble and the surrounding bulk liquid. This period is referenced in the literature /3/ as hydrodynamic bubble growth.

After this period, shorter than 1 msec, the bubble growth is governed by heat conduction in the liquid, due to the potential difference ΔT_{sat} between the liquid temperature and the temperature at the phase interface (fig. 2b). It is assumed that the temperature inside the bubble and respectively at the phase interface is equal to the saturation temperature corresponding to the vapor pressure inside the bubble. This temperature difference guarantees the transport of latent heat, necessary for the evaporation. For this description of the problem, the temperature difference at the phase interface according to the kinetic theory is neglected. During the subsequent bubble growth, the pressure of the liquid is kept nearly constant by means of a metal bellows.

Microgravity conditions are necessary to produce and observe large bubbles, which are not removed by buoyancy forces from the location of nucleation. Furthermore, the temperature field around the bubbles is not disturbed by buoyancy induced convection. Thus the experimental results can be compared with the idealized theoretical formulation of the problem.

Formulation of the Problem for Heat Conduction

The formulation of the problem is similar to that one suggested by Scriven /4/. A spherical bubble, which grows in a quiescent liquid with initial uniform temperature distribution and infinite extent, is assumed. The conservation equations for this problem are as follows.

Equation of Continuity

The equation of continuity is given by eq. (2).

$$\frac{\partial \rho_l}{\partial t} = -\frac{\partial}{\partial r}\left(u(r,t)r^2\right) \tag{2}$$

For constant liquid density this equation can be integrated and results in eq. (3).

$$u(r,t)r^2 = C(t) \tag{3}$$

where r is the radial coordinate of a system originated in the bubble center, $u(r,t)$ is the velocity of displacement of the liquid caused by the ratio between liquid and vapor density. Thus the liquid around the bubble is displaced. The radial velocity of the liquid $u(r,t)$ can be calculated by a mass balance at the liquid vapor interface, given as:

$$\frac{d}{dt}\left(\frac{4}{3}\pi R^3 \rho_v\right) = 4\pi R^2 \rho_l\left[\dot{R} - u(R,t)\right] \tag{4}$$

R is the radius of the bubble and $\dot{R}$ is the velocity of the bubble surface, i.e. the bubble growth rate. For constant liquid density eq. (4) can be solved for $u(R,t)$.

$$u(R,t) = \frac{\rho_l - \rho_v}{\rho_l}\dot{R} = \varepsilon \dot{R} \tag{5}$$

Substituting eq. (5) in eq. (3) and solving for the integration constant $C(t)$ results in eq. (6).

$$ur^2 = \varepsilon \dot{R} R^2 \tag{6}$$

Equation of Motion

The equation of motion is given, for example by Scriven /4/, in the following form

$$\frac{p_v - p_l - 2\sigma/R}{\varepsilon \rho_l} = R\ddot{R} + \frac{3}{2}\dot{R}^2 + 4\eta\frac{\dot{R}}{R} \tag{7}$$

Other authors for example /12/ or /13/ call this equation the „extended Rayleigh equation" but neglect the density factor ε, which is assumed to be unity.

Equation of Energy Flow

For this problem with spherical symmetry, the energy balance is given in eq. (8). In this equation the fluid is thought to be incompressible and the thermal properties are constant.

$$\frac{\partial T}{\partial t} + u\frac{\partial T}{\partial r} = a\left(\frac{\partial^2 T}{\partial r^2} + \frac{2}{r}\frac{\partial T}{\partial r}\right) \tag{8}$$

Together with eq. (6) for the radial velocity in the fluid eq. (8) yields to:

$$\frac{\partial T}{\partial t} = a\left(\frac{\partial^2 T}{\partial r^2} + \frac{2}{r}\frac{\partial T}{\partial r}\right) - \frac{\varepsilon R^2 \dot{R}}{r^2}\frac{\partial T}{\partial r} \tag{9}$$

Boundary Conditions

The coupling between the bubble growth and the energy balance in the liquid is given by the energy boundary condition at the liquid vapor interface. The latent heat for evaporation is provided by heat conduction. The heat available for the evaporation can be calculated with the liquid temperature gradients at the phase interface. The evaporated mass can be determined with the latent heat of evaporation Δh which is well known for R11. Eq. (10) is the energy boundary condition at the bubble surface.

$$-\lambda\left(\frac{\partial T}{\partial r}\right)_{r=R} = \frac{\Delta h \dot{m}}{4\pi R^2} \tag{10}$$

A further boundary condition at the bubble surface is the temperature at the phase interface given in eq. (11)

$$T_{r=R} = T_{sat}(p_v) \tag{11}$$

The boundary condition for the liquid at $r \to \infty$ is given by:

$$T(r \to \infty, t) = T_l \tag{12}$$

This boundary condition is justified by the fact that the bubble and the boundary layer is small compared to the size of the test cell.

The Kinetic Theory

The calculation of the mass flow rate over the liquid vapor interface can be derived from the kinetic theory, according to Hertz /5/ and Knudsen /6/. The background of this theory is, that all molecules striking the liquid vapor interface change the phase either from liquid to vapor or the reverse way from the vapor to the liquid. Molecules colliding with molecules of the contrary phase are reflected. But in this case the other molecule, that originally would have changed the phase, is also reflected and remains in the initial phase. In summary, each molecule striking the liquid vapor interface can be counted as a molecule changing the phase. The number of molecules striking the phase interface can be calculated according to the kinetic theory of gases. For the vapor phase eq. (13) gives the mass of the molecules approaching the phase interface within a certain time. This equals in the condensing mass flow.

$$\dot{m}_{cond} = A\rho_v\sqrt{\frac{k}{2\pi m^*}}\sqrt{T_v} \tag{13}$$

Important is, that T_v is the vapor temperature at the phase interface and ρ_v the corresponding density of the saturated vapor.

The calculation of the evaporating mass flow is based on the following assumption. At the phase interface evaporation and condensation usually takes place at the same time. In case of saturation the evaporating and condensing mass flow rates are equal. Therefore the evaporating mass flow can be calculated by using the eq. (13) for the condensing one. In this case the temperature of the liquid and the saturated vapor density calculated with the liquid temperature has to be used. With eq. (14) and the according temperature the evaporating mass flow rate can be calculated.

$$\dot{m}_{evap} = A\rho_{sat,v}(T_l)\sqrt{\frac{k}{2\pi m^*}}\sqrt{T_l} \qquad (14)$$

In the case of nearly equilibrium, the net mass flow over a liquid vapor interface is the difference between the two mass flows. According to the temperature relation at the phase interface either evaporation or condensation is dominant. The net mass flow over the liquid vapor interface is given by:

$$\dot{m} = 4\pi R^2 \sqrt{\frac{k}{2\pi m^*}}\left(\rho_{sat,v}(T_l)\sqrt{T_l} - \rho_v\sqrt{T_v}\right) \qquad (15)$$

Many researchers, reviewed in /7/ and /8/, tried to verify this theory by using different measurement techniques. In most measurements the mass flow rate predicted by the theory was not reached in the experiment. The evaporation and condensation coefficients β_e and β_c representing the ratio of experimental mass flow rate to theoretical mass flow rate, were introduced. The values of the coefficients vary over decades. However newer theoretical research /9/ seems to confirm that the theory, expressed in eq. (15), is incorrect and that there exists a limit for each fluid based on the structure of the molecules. The calculations by molecule dynamics show, that the coefficients β_e and β_c are not only based on the insufficiency of experiments but much more on the insufficiency of the theory, which does not take into account real molecules and its behavior at the liquid vapor interface. By introducing the coefficients eq. (15) results in eq. (16), which represents the realistic equation for bubble growth according to the kinetic theory.

$$\dot{R} = \frac{1}{\rho_v}\sqrt{\frac{k}{2\pi m^*}}\left(\beta_e\rho_{sat,v}(T_l)\sqrt{T_l} - \beta_c\rho_v\sqrt{T_v}\right) \qquad (16)$$

EXPERIMENTS

Experiments on IML 2

During the IML 2 Spacelab mission this experiment was conducted in the ESA multiuser facility BDPU. A special Test Container was designed for our experiment, using standard interfaces of the facility for power supply, experiment control and data acquisition as well as the optical observation of the facility. This was the first time that undisturbed bubble growth could be observed over a very long time. The results of this mission look very promising. However, the data base for the evaluation was not completed, when this paper was prepared. So unfortunately no results of the IML 2 mission itself can be presented in this paper.

Experiments in JAMIC Drop Shaft

But during the preparations of the Spacelab mission we had the chance to perform several experiments in other facilities. First experiments with a sufficient microgravity level for experiments with free vapor bubbles were conducted in the JAMIC drop shaft. The principle of free fall is used for the compensation of earth gravity. The available microgravity time in the drop shaft (depth app. 700 m, free fall app. 490 m) is 10 seconds. The volume that can be used for experimental hardware is about 1 m^3 and the maximum weight of the payload is about 1000 kg. The drop shaft is located on Hokkaido, the northernmost of the Japanese main islands. Thanks to the German Japan cooperation in microgravity research we had the chance to perform nine drops in October and November 1992. More details concerning the technical details of JAMIC are given in the user guide /10/.

Experiments in the Bremen Drop Tower

Another series of experiments, with about 30 drops up to now, could be conducted in the ZARM drop tower Bremen. Like at JAMIC the principle of free fall is used for the compensation of the earth gravity. The height of the tower is about 130 m, with 110 m respectively 4.7 sec for free fall. These experiments were sponsored by ESA. More details concerning the technical details of the drop tower are given in /11/.

Sounding Rocket Experiment

Furthermore we could fly an experiment for this research project on a sounding rocket. The earth gravity is compensated during a ballistic flight trajectory of a rocket after the rocket motors are burned out and pushed away. The time with microgravity conditions is app. 360 sec with an apogee height of 250 km. The experiment is controlled from ground by predefined telecommands. The course of the experimental run is observed by several video channels and the data are transferred by telemetry to the ground station. The rocket is launched near Kiruna, a city in Northern Sweden.

Experimental Hardware

The principle for the various experimental set ups was the same. However small differences occur in the structural and some design features. In the following only the principle of the experiments shall be explained. The hardware for the drop experiments was designed and built by ourselves. The hardware for the sounding rocket was built by DASA ERNO and for the BDPU by DASA Dornier and Ferrari.

The main component of the fluid system is the experiment cell. The temperature of the cell is controlled by means of two Peltier

elements. In the center of the cell the miniaturized heater (i.e. a thermistor) was located. Several thermistors for temperature measurement were grouped around it. A separate volume compensation and pressure control vessel was connected to the cell. Inside this vessel a metal bellows separates the fluid volume from an air volume whose counterpressure can be controlled by two solenoid valves and an adjustable needle valve operated by a special control loop. One of these valves was connected to a pressure bottle. By opening this valve, the pressure increase could be controlled. The other one was connected with the ambient for a pressure decrease. The gradient could be controlled by adjusting the needle valve.

The growth of the vapor bubble is observed in two perpendicular directions. Alternative high speed cameras and video cameras with video tape recorders were used for image recording. For the investigation of the temperature field around the bubbles a Wollaston type interferometer (drop experiments) or a Point Diffraction Interferometer (BDPU) was available. A computer was used for experiment control and data acquisition. In the drop experiments a special designed software for experimental control was necessary to use the short time of microgravity conditions to a maximum extent.

Experiment Program

In the drop shaft we performed nine drops at liquid temperature between 35 and 50 °C with different supersaturations, ranging from 200 to 400 mbar. Up to now an overall number of 30 drops had been available in the drop tower with liquid temperature levels of 35, 50, 65 and 80 °C. Accordingly the supersaturation pressures ranged from 50 mbar up to 500 mbar.

EVALUATION

Bubble Growth Rates

For our problem the conservation equations for bubble growth cannot be solved in a closed form. In the past several authors gave approximate solutions for the bubble growth controlled by heat conduction. The form of the equations results from the solution of the energy balance for non steady heat conduction.

Forster and Zuber /12/ give for the case of asymptotic bubble growth:

$$R(t) = \pi^{0.5} Ja\,(at)^{0.5} \tag{17}$$

with the Jakob number Ja defined as

$$Ja = \frac{c_l\,\rho_l}{\Delta h\,\rho_v}\,\Delta T_0$$

including the initial isobaric supersaturation ΔT_0 of the liquid, the most important experimental parameter.

The solution of Plesset and Zwick /13/ for the asymptotic case results in the same relation with a constant factor about 10 % higher.

$$R(t) = \left(\frac{12}{\pi}\right)^{0.5} Ja\,(at)^{0.5} \tag{18}$$

The solution of Scriven /4/ for high supersaturations, which can be applied for our problem, is the same as the solution given by Plesset and Zwick.

As later demonstrated these asymptotic solutions are in poor agreement with the experimental results. So a numerical model for the case of bubble growth controlled by heat conduction was developed.

Numerical model

In the numerical solution spherical symmetry is assumed. The energy eq. (9) was discreted for finite radial elements Δr and finite time steps (Δt). The new temperature (T^1) of each element can be explicitly calculated from the preceding temperatures (T^0) according to the following eq. 19.

The index n denotes the temperature of the n-th element. A non equidistant spacing is used. The mesh is stretched with increasing distance from the bubble surface. In this case the steep temperature gradient around the bubble is considered and the computing time can be minimized. The calculation always starts from the bubble surface. After each time step the new temperature field has to be calculated using the new bubble radius.

The boundary conditions are given in chapter **2.3.** The initial conditions of the calculation are given by the critical nucleation radius for the supersaturation and the temperature of the undisturbed liquid. Thus the initial conditions can be formulated in the following way.

$$R(t=0) = \frac{2\sigma}{\Delta p_0}$$

$$\dot{R}(t=0) = 0$$

$$T(r, t=0) = T_0$$

The energy balance at the phase interface (eq. 10) gives the bubble growth rate $\dot{R}$ and subsequently the radius R at each time step. This results in the R-t curve for each bubble.

Evaporation and Condensation Coefficients

For the calculation of the evaporation and condensation coefficient the liquid temperature at the phase interface is necessary, which could not be measured directly. So the

$$T_n^1 = T_n^0 + \Delta t \cdot \left[-\left(r_n - \frac{\Delta r_n}{2}\right)^2 \frac{T_n^0 - T_{n-1}^0}{\Delta r_n - \Delta r_{n-1}} + \left(r_n + \frac{\Delta r_n}{2}\right)^2 \frac{T_{n+1}^0 - T_n^0}{\Delta r_{n+1} + \Delta r} \right] - \Delta t \cdot \left(1 - \frac{\rho_v}{\rho_l}\right) \frac{R(t)^2 \dot{R}(t)}{r_n^2} \left(\frac{T_n^0 - T_{n-1}^0}{\Delta r_n + \Delta r_{n-1}} + \frac{T_{n+1}^0 - T_n^0}{\Delta r_n + \Delta r_{n+1}} \right) \tag{19}$$

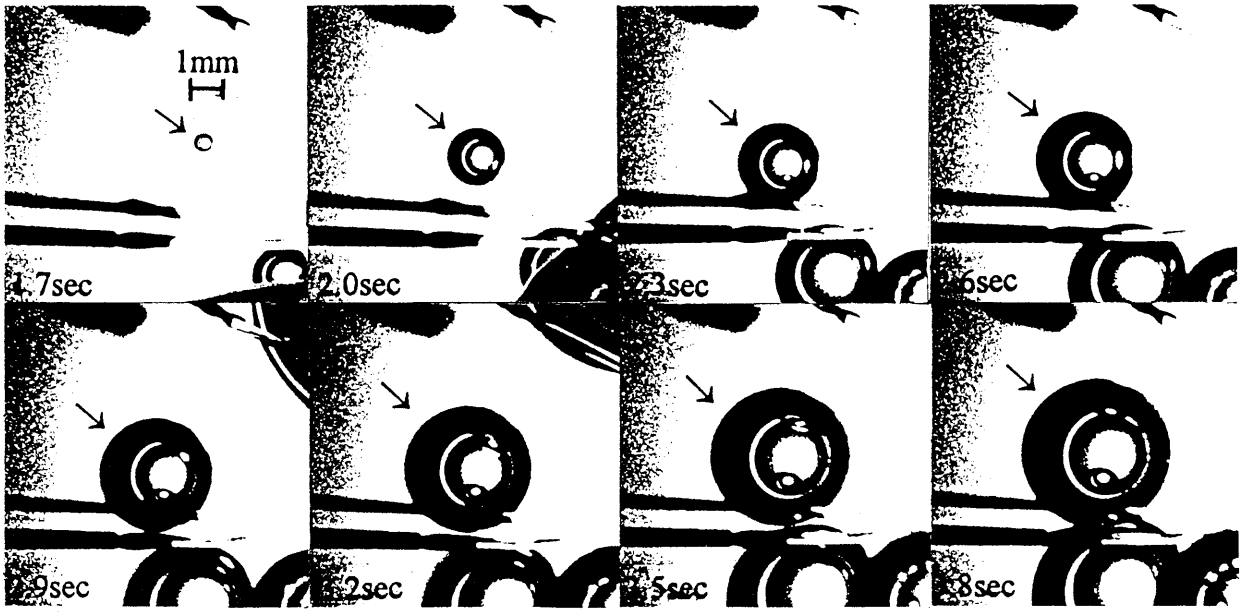

Fig. 4: Growing vapor bubble under microgravity, bubble marked with '→' secondary bubble resulting from a coalescence, T_l = 35 °C, Δp_{sat} = 0.140 bar

previously described numerical model is used for the calculation of this temperature. From the measured *R-t* curve and the energy balance at the phase interface (eq. 10) the temperature gradient at the bubble surface is determined. This gradient and the liquid temperature are now used as boundary conditions for the numerical calculations. From that the interface temperature is determined at each time step.

To calculate the evaporation and condensation coefficient separately, we make the calculation with eq. (16) twice for different points of the bubble growth curve. The other variables are known by the experiment or the numerical calculation. This is performed several times for one growing bubble in order to minimize errors.

RESULTS OF THE EXPERIMENTS

General results

In the beginning one of our main problems was the maximum achievable supersaturation. We observed uncontrolled nucleation at the walls when reducing the pressure below the saturation pressure. Finally we achieved isothermal supersaturation pressures greater than 1 bar, before uncontrolled nucleation occurred. Nevertheless for the experiment we selected no higher supersaturation than 0.5 bar to limit the dynamic of the bubble growth. In fig. 3 a typical pressure time diagram of one drop is shown together with the saturation pressure, calculated from the measured liquid temperature. The decrease of saturation pressure, marked with (*) is due to the temperature decrease near the bubble surface measured by the thermistor, which is used for the calculation of the saturation pressure.

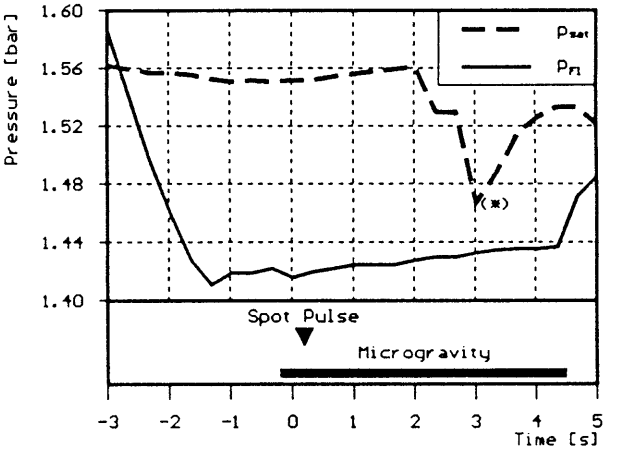

Fig. 3: Typical pressure time diagram of one drop (T_l = 30 °C)

Another critical problem was the optimum setting of the spot heater pulse time. We desired to generate only one vapor bubble. Therefore the pulse time and temperature set of the heater were optimized in 1g reference experiments before the microgravity experiments. Finally we worked with pulse times of the order of 150 msec. But even with these optimized settings, only sometimes a single vapor bubble could be generated. In most runs a number of bubbles was generated by the heating pulse. We also observed that the heat pulse time, necessary for nucleation, was shorter under normal gravity than under microgravity conditions.

The data, especially the high speed films (400 frames per second) and video tapes, recorded during the experiments,

contain excellent basic material for the analysis of the bubble growth. The quantitative evaluation of the material is very time consuming, due to the fact that the evaluation of the films has to be done picture by picture with a digital image processing system.

One interesting phenomena which we could also observe during several runs but not evaluate until now is the coalescence of vapor bubbles. Sometimes when several vapor bubbles are generated some vapor bubbles coalesce. After the coalescence the resulting vapor bubble is oscillating with a certain frequency. More over new bubbles are generated at the first retraction of the big oscillating vapor bubble. The coalescence process, the oscillation of the combined bubble and the generation of the secondary bubbles will be evaluated separately.

Bubble Growth

A typical sequence of a vapor bubble growing at low Jakob Numbers is shown in fig. 4. The bubble marked with an arrow is the result of the coalescence of two bigger vapor bubbles. This bubble does not result from a nucleation on the surface of the spot heater. The pictures shown here are enlarged from a high speed film (400 fps) taken during a drop at ZARM drop tower. Fig. 5 demonstrates the measured radius time curve for this bubble. The fluid temperature was 35 °C with a supersaturation of app. 140 mbar, that equals in an isobaric ΔT_{sat} of 2.7 K and a Jakob number of $Ja = 2.5$.

Fig. 5 also shows the curve calculated with the analytical solution given by Scriven, which is in this case identical with the solution of Plesset and Zwick. Scriven predicted like Forster and Zuber slower growth rates than measured in the experiment. However the numerical calculated growth rates are in good agreement with the measurements.

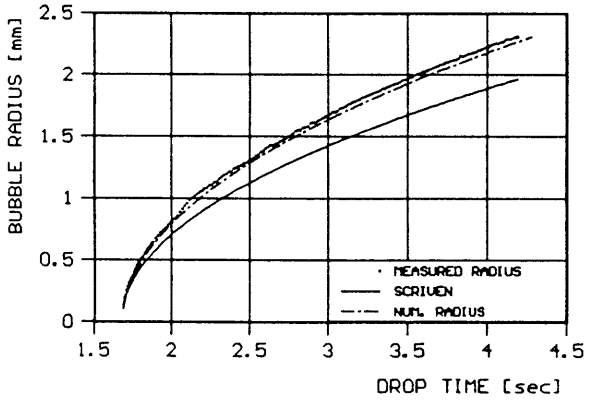

Fig. 5: R,t curve of a growing vapor bubble
$T_l = 35$ °C, $\Delta p_{sat} = 0.140$ bar, Ja = 2.7 (ZB7B15)

Fig. 6 shows the radius time curve for a bubble, directly initiated with the heating pulse. The normal calculation is in poor agreement with the measured R,t - curve. The growth rate at the beginning is very high. This effect can be explained with the additional heat, produced by the spot heater. This initial heat source is considered in our program by a volumetric heat source added to the right hand side of eq. 19 in the case of nucleation on the spot heater surface. The resulting R,t - curve is also shown in fig. 6. The calculation with the additional heat source is in good agreement with the measurement.

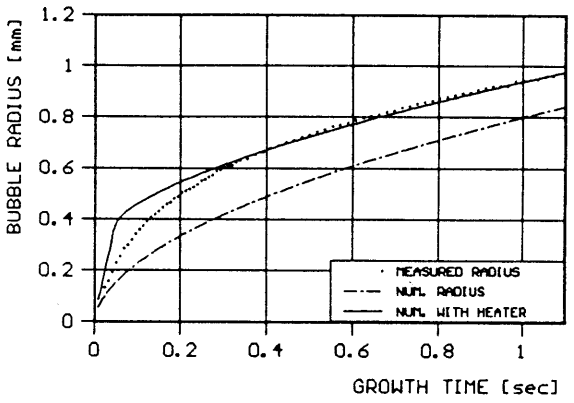

Fig. 6: R,t curve of a vapor bubble initiated with spot heater

$T_l = 50$ °C, $\Delta p_{sat} = 0.160$ bar, Ja = 1.4 (ZA3B2)

Figures 7, and 8 show some more radius time curves for different liquid states and supersaturations. The data for fig. 8 are from the TEXUS flight. The bubble was observed for more than 14 sec and the numerical model predicts the bubble growth very well.

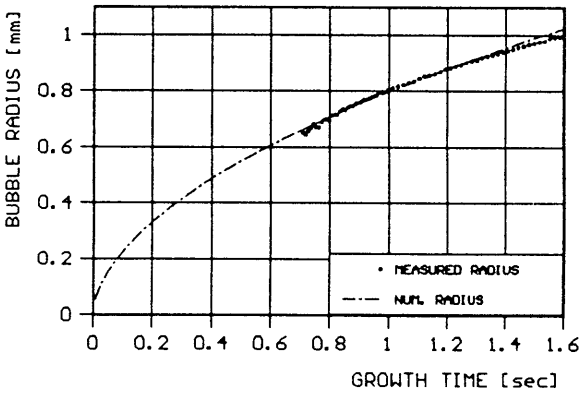

Fig. 7: R,t curve of a growing vapor bubble

$T_l = 50$ °C, $\Delta p_{sat} = 0.160$ bar, Ja = 1.4 (ZA3B3)

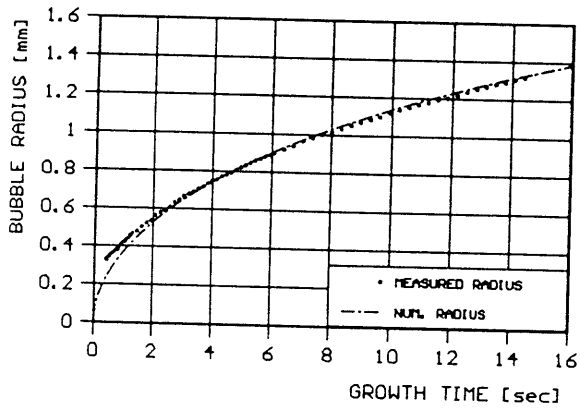

Fig. 8: R,t curve of a growing vapor bubble
T_l = 40 °C, Δp_{sat} = 0.040 bar, Ja = 0.5 (T31B6)

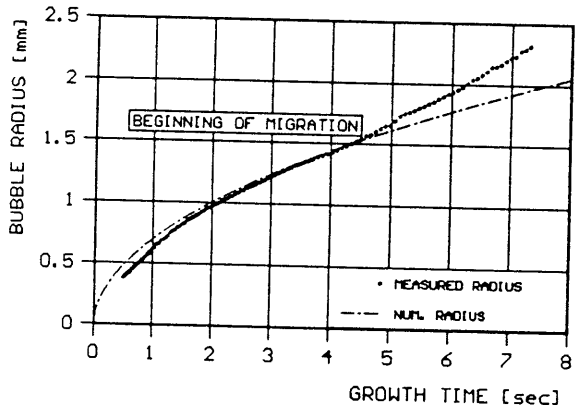

Fig. 9: R,t curve of a bubble starting to migrate at 4.5 sec
T_l = 40 °C, Δp_{sat} = 0.040 bar, Ja = 0.5 (T31B14)

One example for the R,t - curve of a slow migrating bubble is given in fig. 9. The bubble starts migrating after app. 4.5 sec. Consequently the bubble growth is enhanced by the increase of the temperature gradient at the liquid vapor interface. Effects like this are not considered in our program. Therefore such bubbles are not considered for the determination of the kinetic coefficients.

Kinetic Coefficients

As mentioned above, the liquid temperature at the phase interface has to be calculated with the numerical model. The temperature inside the bubble is assumed to be homogeneous and equal to the saturation temperature corresponding to the system pressure. The error introduced by the pressure difference according to eq. (1) is negligible small in our case, were the typical temperature differences at the phase interface are of the order of 0.5 K. Using eq. (15) twice at different times, the system of the two equations can be solved for β_e and β_c. This feature is implemented in the evaluation program.

The variation of the evaporation and condensation coefficient during bubble growth is shown in fig. 10 for one bubble. The evaporation coefficient is nearly equal to the condensation coefficient. The coefficients start at high values and drop down to a nearly constant value after the initial phase. A typical temperature difference for this period is 0.5 K. A summary of the coefficients obtained from the experiments is given in fig. 11. The evaporation and the condensation coefficients for different vapor bubbles lie between $1 \cdot 10^{-4}$ and $1 \cdot 10^{-3}$.

The largest uncertainty is caused by the calculation of the liquid temperature at the bubble surface. These uncertainties can be reduced by measuring the temperature field around a bubble with an interferometer. First experiments with a Wollaston type interferometer in the drop shaft show very promising results.

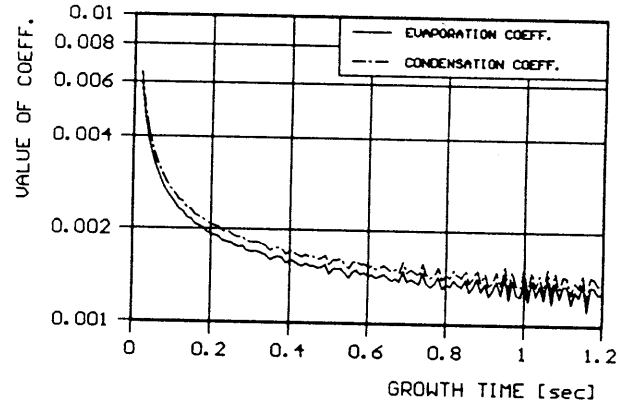

Fig. 10: Evaporation and condensation coefficient of a growing vapor bubble

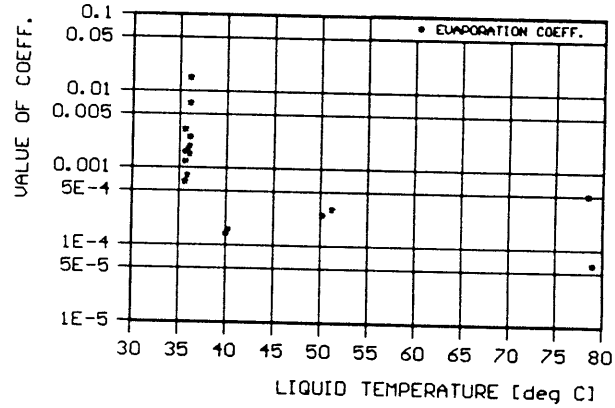

Fig. 11: Evaporation coefficients as a function of liquid temperature

CONCLUSIONS

A series of drop shaft / drop tower experiments and a TEXUS experiment provided data about the growth of free vapor bubbles in a homogenous supersaturated liquid. The growth of the bubbles was observed up to 14 sec. During a Spacelab

experiment the bubble growth and collapse were observed over a very long period. The bubble growth rates in R11 were determined at various liquid temperature levels. Our experimental set up allowed the control of the liquid supersaturation before the bubbles were initiated at a miniaturized heater. Therefore even a variation of the supersaturation was possible.

The measured curves for vapor bubble growth are in good agreement with our numerical simulation. The numerical model for the heat conduction controlled bubble growth is based on the energy balance. The model takes into account the displacement of the liquid during the bubble growth.

With the same code and the experimental values of the bubble growth curve, the temperature at bubble interface is determined. With this temperature and the temperature inside the bubble the mass flow through the liquid vapor interface and subsequently the evaporation and the condensation coefficients were determined. Their values according to the kinetic theory are between $1 \cdot 10^{-4}$ and $1 \cdot 10^{-3}$ for R11.

There are some uncertainties in the calculation of the liquid temperature at the phase interface. Therefore an interferometer was used in drop experiments in order to measure the temperature around the bubble more accurately. First pictures of the interferometer look very promising. The experiments will be continued under microgravity conditions with the alternative refrigerant R134a. Furthermore it is important to study the influence of inert gas on the evaporation and condensation kinetics in future. A reflight of the experiment flown on IML 2 is scheduled on the LMS mission of NASA in June 1996. More experiments with an substantially extended time scale will be possible on this mission

NOMENCLATURE

A	surface
C	constant
k	Boltzmann constant
m	mass
m^*	molecular mass
$\dot{m}$	mass flow
p	pressure
r	radial coordinate
R	bubble radius
$\dot{R}$	bubble growth rate
t	time
T	temperature
u	liquid velocity

Greek Symbols

β	evaporation and condensation coefficient
λ	thermal conductivity
ρ	density
σ	surface tension
Δ	difference

Subscripts

c	condensation
e	evaporation
l	liquid
n	number of element
sat	saturation
v	vapor

REFERENCES

/1/ P. Dergarabedian, *The rate of growth of vapor bubbles in superheated water;* J. Apl. Mech., vol. 20, pp. 537 - 545, (1953);

/2/ R. Cole, H. L. Shulman; *Bubble growth rates at high Jakob numbers;* Int. J. Heat and Mass Transfer, vol. 9, pp. 1377 - 1390, (1966);

/3/ S. van Stralen, R. Cole; *Boiling Phenomena;* Hemisphere Publishing Corporation, Washington, (1979);

/4/ L. E. Scriven, *On the dynamics of phase growth;* Chemical Eng. Science, vol. 10, no. 1/2, pp. 1 - 13, (1959);

/5/ H. Hertz; Ann. Phys.; 17 (1882), p. 193;

/6/ M. Knudsen, Ann. Phys., 29 (1909), p. 179;

/7/ B. Paul; *Compilation of Evaporation Coefficients;* ARS Journal, vol. 32, no. 9, pp. 1321 - 1328, (1962);

/8/ G. M. Pound, *Selected Values of Evaporation and Condensation Coefficients for Simple Substances;* J. Phys. Chem. Ref. Data, vol. 1, no. 1, pp. 135 - 146, (1972);

/9/ M. Matsumoto, K. Yasuoka, Y. Kataoka; *Molecular Simulation of Evaporation and Condensation at the Liquid Vapor Interface;* Proc. 14th Japan Symp. on Thermophysical Properties;, Japan, pp. 143 - 146, (1993);

/10/ *Japan Microgravity Center User's Guide;* Japan Microgravity Center (JAMIC), Japan Space Utilization Promotion Center (JSUP), October (1991);

/11/ *Drop Tower „Bremen", User Manual;* vol. 2.2 (1992);

/12/ H. K. Forster, N. Zuber; *Growth of a Vapor Bubble in Superheated Liquid;* J. of Appl. Phys. vol. 25, pp. 493 - 500, (1954);

/13/ M. S. Plesset, S. A. Zwick; *The Growth of Vapor Bubbles in Superheated Liquid;* J. of Appl. Phys., vol. 25, pp. 493 - 500, (1954);

ACKNOWLEDGMENT

We like to express our appreciation to all, who makes this research possible. Especially we thank the team of JAMIC, the team of ZARM and all peoples and companies involved in the TEXUS project. Finally we want to express our thanks to the European Space Agency ESA for the flight opportunities and to the German Space Agency DARA for the financial support of this project.